HAL
archives-ouvertes.fr

Evidence for the Formation of a Covalent Thiosulfinate Intermediate with Peroxiredoxin in the Catalytic Mechanism of Sulfiredoxin

Xavier Roussel, Guillaume Béchade, Alexandre Kriznik, Alain Van Dorsselaer, Sarah Sanglier-Cianferani, Guy Branlant, Sophie Rahuel-Clermont

▶ **To cite this version:**

Xavier Roussel, Guillaume Béchade, Alexandre Kriznik, Alain Van Dorsselaer, Sarah Sanglier-Cianferani, et al.. Evidence for the Formation of a Covalent Thiosulfinate Intermediate with Peroxiredoxin in the Catalytic Mechanism of Sulfiredoxin. Journal of Biological Chemistry, American Society for Biochemistry and Molecular Biology, 2008, 283 (33), pp.22371-22382. <10.1074/jbc.M800493200>. <hal-01652689>

HAL Id: hal-01652689
https://hal.univ-lorraine.fr/hal-01652689

Submitted on 30 Nov 2017

HAL is a multi-disciplinary open access archive for the deposit and dissemination of scientific research documents, whether they are published or not. The documents may come from teaching and research institutions in France or abroad, or from public or private research centers.

L'archive ouverte pluridisciplinaire **HAL**, est destinée au dépôt et à la diffusion de documents scientifiques de niveau recherche, publiés ou non, émanant des établissements d'enseignement et de recherche français ou étrangers, des laboratoires publics ou privés.

THE JOURNAL OF BIOLOGICAL CHEMISTRY VOL. 283, NO. 33, pp. 22371–22382, August 15, 2008
© 2008 by The American Society for Biochemistry and Molecular Biology, Inc. Printed in the U.S.A.

Evidence for the Formation of a Covalent Thiosulfinate Intermediate with Peroxiredoxin in the Catalytic Mechanism of Sulfiredoxin*[S]

Received for publication, January 18, 2008, and in revised form, May 28, 2008 Published, JBC Papers in Press, June 14, 2008, DOI 10.1074/jbc.M800493200

Xavier Roussel[‡1], Guillaume Béchade[§1], Alexandre Kriznik[‡], Alain Van Dorsselaer[§], Sarah Sanglier-Cianferani[§], Guy Branlant[‡2], and Sophie Rahuel-Clermont[‡3]

From the [‡]Unité Mixte de Recherche, CNRS-UHP 7567, Maturation des Acide Ribonucléique et Enzymologie Moléculaire, Nancy Université, Faculté des Sciences, Bld. des Aiguillettes, BP 239, Vandoeuvre-lès-Nancy 54506, France and the [§]Unité Mixte de Recherche, CNRS-ULP 7178, Laboratoire de Spectrométrie de Masse Bio-Organique, Institut Pluridisciplinaire Hubert Curien, Département Sciences Analytiques, Ecole de Chimie, Polymères et Matériaux, 25, rue Becquerel, Strasbourg 67087, France

The typical 2-Cys peroxiredoxins are thiol-peroxidases involved in the physiology of hydrogen peroxide not only as a toxic but also as a signaling molecule. Coordination of these functions depends on the sulfinylation of the catalytic Cys, a modification reversed by ATP-dependent sulfiredoxin, which specifically reduces the sulfinic acid group of overoxidized 2-Cys peroxiredoxins into a sulfenic acid. Sulfiredoxin was originally proposed to operate by covalent catalysis, with formation of a peroxiredoxin-sulfiredoxin intermediate linked by a thiosulfinate bond between the catalytic Cys of both partners, a hypothesis rejected by a study of the human enzyme. To settle the argument, we investigated the catalytic mechanism of *Saccharomyces cerevisiae* sulfiredoxin, by the characterization of the nature and kinetics of formation of the protein species formed between sulfiredoxin and its substrate in the presence of ATP, using mutants of the non-essential Cys residues of both proteins. We observed the formation of a dithiothreitol-reducible peroxiredoxin-sulfiredoxin species using SDS-PAGE and Western blot analysis, and its mass was shown to correspond to a thiosulfinate complex by high resolution mass spectrometry coupled to liquid chromatography. We next measured indirectly and directly a rate constant of formation of the thiosulfinate species of $\sim$2 min^{-1}, for both wild-type and mutant sulfiredoxins, at least equal to the steady-state rate constant of the reaction, with a stoichiometry of 1:1 relative to peroxiredoxin. Taken altogether, our results strongly argue in favor of the formation of a covalent thiosulfinate peroxiredoxin-sulfiredoxin species as an intermediate on the catalytic pathway.

Reactive oxygen species, including hydrogen peroxide originating both from exogen and endogen sources, are compounds deeply involved in cellular physiology. They can result in either toxic or beneficial effects through chemical modification of cellular components. Sulfinylation of a protein cysteine thiol was considered to be a biologically irreversible event *in vivo* until the discovery of new enzymatic sulfinyl reductase activities referred to as sulfiredoxin (Srx)[4] (1) and sestrins (2), capable of reducing a sulfinic acid group -SO_2H (sulfur oxidation number +II) into a sulfenic acid -SOH (oxidation number 0). The strong interest toward the elucidation of the molecular and structural enzymology of these enzymes lies in their potential regulatory functions affecting the bipolar nature of H_2O_2 as a toxic and a carcinogen, and as a signaling molecule (3–5).

In these mechanisms specific to eukaryotic organisms, a family of thiol-peroxidases susceptible to Cys sulfinylation, the peroxiredoxins (Prx), plays a central role and constitutes the specific substrate of Srx and sestrins (2, 6). Typical 2-Cys Prx (2-Cys-Prx) represents a class of peroxidase distinct from catalase and glutathione peroxidase, the functional unit of which is structured as a symmetrical homodimer. Typical 2-Cys-Prxs reduce H_2O_2 by oxidation of the N-terminal catalytic Cys (C_P) to a sulfenic acid intermediate, then recycled by disulfide formation with a regenerating Cys (C_R) located on the symmetrical subunit, finally coupled to reduction by thioredoxin. Furthermore, Prxs have been proposed to participate in the transduction and regulation of H_2O_2-mediated cell signaling (7).

The modulation of Prx activity by post-translational modification adds another layer to the potential regulations of H_2O_2 effects in eukaryotic cells. The Prx peroxidase activity is inhibited by Thr phosphorylation (8). In addition, eukaryotic 2-Cys-Prxs have been described to be susceptible to the oxidation of the catalytic Cys to a higher level, the sulfinic acid state, during the catalytic cycle, by a mechanism of escape of the reactive sulfenic acid intermediate (9). This overoxidation of 2-Cys-Prx, also observed *in vivo*, not only abolishes peroxidase activity but

* This work was supported in part by the CNRS, the University of Nancy I, the Institut Fédératif de Recherche 111 Bioingénierie, and by the French Agence Nationale de la Recherche (Program ANR-06-BLAN-0369). The costs of publication of this article were defrayed in part by the payment of page charges. This article must therefore be hereby marked "*advertisement*" in accordance with 18 U.S.C. Section 1734 solely to indicate this fact.

[S] The on-line version of this article (available at http://www.jbc.org) contains supplemental text and Figs. S1–S5.

[1] Supported by the French Research Ministry.

[2] To whom correspondence may be addressed. Tel.: 33-3-83-68-43-04; Fax: 33-3-83-68-43-07; E-mail: guy.branlant@maem.uhp-nancy.fr.

[3] To whom correspondence may be addressed. Tel.: 33-3-83-68-43-12; Fax: 33-3-83-68-43-07; E-mail: sophie.rahuel@maem.uhp-nancy.fr.

[4] The abbreviations used are: Srx, sulfiredoxin; Prx, peroxiredoxin; 2-Cys-Prx, two-cysteine peroxiredoxin; C_P, 2-Cys-Prx catalytic Cys; C_R, 2-Cys-Prx regeneration Cys; DTT, 1,4-dithiothreitol; IAM, iodoacetamide; LC-MS, reversed-phase liquid chromatography coupled to mass spectrometry; ^{me7}Guo, methyl-7-guanosine; MES, 2-(*N*-morpholino)ethanesulfonic acid; NTR, *E. coli* NADPH thioredoxin reductase; PNP, His-tagged purine nucleoside phosphorylase from *E. coli*; $PrxSO_2$, overoxidized *S. cerevisiae* His-tagged peroxiredoxin Tsa1; Trx, *E. coli* thioredoxin 1; FWHM, full width at half-maximum.

also stabilizes high molecular weight forms of Prx, which show chaperone-like activities. Therefore, sulfinyl reductase activities can potentially regulate several aspects of H_2O_2 physiology involving Prx in eukaryotes, by restoring the native state of 2-Cys-Prx: 1) in the "floodgate" theory (9), sulfinylation/sulfinyl reduction would be associated with the requirement of temporary and/or local inactivation of Prx peroxidase activity to allow the transmission of H_2O_2-mediated signal; 2) as proven in *Schizosaccharomyces pombe*, Prx overoxidation and its reversion by Srx constitute a redox switch between two signal transduction paths dependent on H_2O_2 concentration (10); and 3) in view of the recently reported chaperone activity induced by overoxidation, sulfinyl reductase would also regulate a switch between oxidative stress conditions, with overoxidized 2-Cys-Prx acting as a cellular protector, and H_2O_2 signaling conditions, with native reduced 2-Cys-Prx acting as redox sensor for example (11). In addition, a new regulator function for human Srx has been proposed, by catalysis of the deglutathionylation of several distinct proteins in response to oxidative stress (12). In support of the role of Srx as part of cellular redox regulation and signaling systems, several studies have shown that expression of Srx is induced under oxidation stress conditions, including yeasts, plants, and mammals (1, 13–15).

Srxs are small proteins of 13–18 kDa generally with a basic character, identified in the genome of some eukaryotes (in plant and algae, metazoans, and fungi) and some cyanobacteria species. They catalyze the ATP-dependent reduction of the overoxidized catalytic Cys C_P (as sulfinic acid) of typical 2-Cys-Prx, with substrate specificity exclusive of other Prx classes or of other proteins possessing a Cys sensitive to overoxidation (*e.g.* glyceraldehyde 3-phosphate dehydrogenase) (6). The Srx activities described so far for mammalian enzymes are slow, with turnover numbers of 0.2– 0.5 min^{-1} (16, 17).

The Srx activity was initially described by Biteau *et al.* (1), on the *Saccharomyces cerevisiae* enzyme, who proposed a catalytic mechanism in which Srx acted first as an ATP-dependent phosphotransferase to activate the sulfinic group of the Prx substrate as a phosphoryl sulfinic intermediate, leading to the release of ADP. In a second step, Srx would act as a reductase through the formation of a PrxSO·SSrx thiosulfinate intermediate involving Srx essential Cys (Cys-99 in mammalian enzymes, Cys-84 in *S. cerevisiae* enzyme), a phosphate group being thus released in this step (Fig. 1*A*). This intermediate would be reduced by thioredoxin or by another thiol reductant, leading to the release of the Prx reduced in the sulfenic acid state and of a mixed disulfide thioredoxin-Srx, followed by recycling of Srx to the reduced form and release of oxidized thioredoxin. In 2006, an alternative mechanism based on a kinetic study of the human enzyme reaction and infirming the reductase role of Srx was supported. In this mechanism, the Prx phosphoryl sulfinic intermediate is directly reduced by a thiol reducer distinct from Srx (17) (Fig. 1*B*).

In the present report, we examined the catalytic mechanism of *S. cerevisiae* Srx. First, we characterized the protein species formed between Srx and its overoxidized 2-Cys-Prx substrate in the absence of added reducer by the use of SDS-PAGE, Western blot, and mass spectrometry coupled to liquid chromatography. Second, to validate the formation of these species as part of the catalytic mechanism, we then designed kinetic approaches aimed at monitoring the kinetics and stoichiometry of the putative steps. To avoid secondary reactions, we used mutants of the non-essential Cys residues of both Srx and the overoxidized Prx. Altogether, our results favor the formation of a covalent thiosulfinate Prx-Srx species as an intermediate of Srx catalytic pathway.

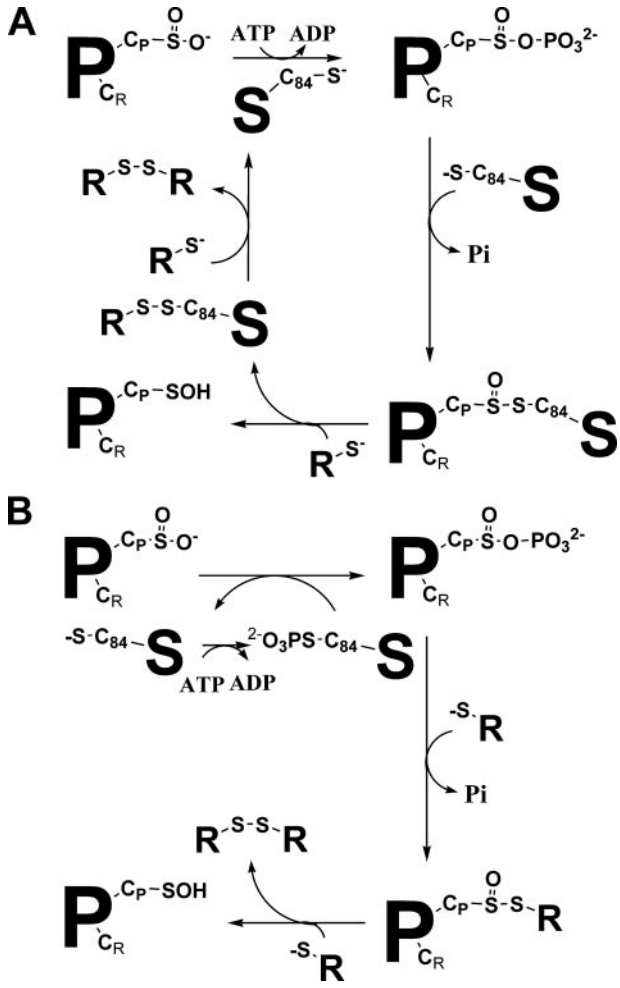

FIGURE 1. **Srx hypothetical catalytic mechanisms.** In hypothesis *A*, Srx catalyzes both the phosphotransferase and the reductase steps by reductive attack of the catalytic Cys on the phosphorylated substrate, leading to a covalent thiosulfinate intermediate with Srx. Subsequent reduction is achieved by an external reducer. In hypothesis *B*, Srx only catalyzes the reductase step by a phosphorylated Srx intermediate. All subsequent reduction steps depend on an external reducer. No covalent intermediate is formed between Srx and the Prx substrate. *P*, Prx; *S*, Srx; C_P, peroxidatic Cys; C_R, regeneration Cys; C_{84}, Srx catalytic Cys; *R*, thiol reducer distinct from Srx.

EXPERIMENTAL PROCEDURES

Materials—Tris was from VWR (West Chester, PA). KCl and $MgCl_2$ were from Merck (Darmstadt, Germany), NADPH was obtained from Roche (Basel, Switzerland), and dithiothreitol (DTT) and ammonium sulfate were from Euromedex (Souffelweyersheim, France). ATP, MES, iodoacetamide (IAM), ammonium hydrogen carbonate, and horse heart myoglobin were from Sigma-Aldrich, and phosphoric acid and H_2O_2 were from Acros Organics (Geel, Belgium). Rabbit antiserum specific for purified *S. cerevisiae* Srx was produced by Centre Lago (Vonnas, France). Mouse antiserum specific for His tag was

from Qiagen (Hilden, Germany), and secondary antisera were obtained from Pierce. Trifluoroacetic, formic acids, and ^{m7}guanosine (^{m7}Guo) were from Fluka. Acetonitrile was obtained from Carlo Erba Reactifs SDS (Val de Reuil, France).

Thioredoxin 1 (Trx) and NADPH thioredoxin reductase (NTR) from *Escherichia coli* were prepared following experimental procedures described previously (18, 19). Purine nucleoside phosphorylase from *E. coli* was expressed from a plasmid derived from pET28b(+) encoding the N-terminal His tag fusion protein of the enzyme (referred to as PNP), obtained by cloning the *deoD* open reading frame amplified by PCR using *E. coli* K12 genomic DNA as template between the NdeI and SacI sites (oligonucleotides not shown). The PNP was produced and purified according to the same procedures as the His-tagged *S. cerevisiae* Prx (see below), and stored as a lyophilizate at −20 °C.

Plasmid Constructions and Preparation of Recombinant S. cerevisiae Srx and Prx Proteins—The plasmid pET20bSrxΣ encoding the *S. cerevisiae* Srx protein was obtained by subcloning the synthetic *srx*Σ open reading frame optimized for expression in *E. coli* (GeneArt AG, Regensburg, Germany), into the pET20b(+) plasmid (Novagen, Merck Chemicals, Darmstadt, Germany) between the NdeI and SacI sites. The plasmid pET28bHTTsa1 encoding the N-terminal His tag fusion protein of *S. cerevisiae* 2-Cys-Prx Tsa1 (referred to as Prx in the following text) was obtained by cloning the *tsa1* open reading frame amplified by PCR (GC-rich system, Roche Applied Science, Basel, Switzerland) using *S. cerevisiae* W303 genomic DNA as template, into the pET28b(+) plasmid between the NdeI and SacI sites. The forward primer contained an NdeI restriction site, and the reverse primer contained an SacI restriction site (sequences of oligonucleotides not shown). The mutant proteins C48A-C106A Srx and C171A Prx were generated by standard PCR site-directed mutagenesis. *E. coli* C41(DE3) [F^- ompT hsdS_B ($r_B{}^-$ $m_B{}^-$) gal dcm (DE3)] (20) transformants containing the wild-type or mutant pET20bSrxΣ were grown at 37 °C for 24 h and 30 h, respectively, in the autoinducible media ZYM-5052 or N-5052 (21), respectively, supplemented with ampicillin (200 mg l^{-1}). Wild-type and mutant Prxs were overexpressed in the same strain transformed by the pET28bHTTsa1 plasmid, by overnight culture at 37 °C in the ZYM-5052 medium supplemented with kanamycin (200 mg l^{-1}).

For Srx purification, cells were harvested by centrifugation, resuspended in a minimal volume of buffer A (100 mM MES pH 6.1) containing 20 mM DTT, and disrupted by sonication. Srx contained in the soluble fraction of the cellular extract was then precipitated by ammonium sulfate at 55% saturation, followed by cation exchange chromatography on a sulfopropyl-Sepharose column connected to a fast protein liquid chromatography system (Amersham Biosciences) equilibrated with buffer A. Srx was eluted by a 0–1 M KCl linear gradient with a step at 350 mM. Final purification of Srx was achieved by hydrophobic chromatography on a phenyl-Sepharose column (Amersham Biosciences) equilibrated with buffer A plus 1 M ammonium sulfate, eluted with a linear 1 to 0 M ammonium sulfate gradient. For Prx purification, cells were harvested by centrifugation, resuspended in a minimal volume of buffer B (20 mM K_2HPO_4, 1 M KCl, pH 7.5) containing 20 mM DTT and disrupted by sonication. Prx contained in the soluble fraction was purified on nickel-Sepharose column equilibrated with buffer B plus 50 mM imidazole, connected to a fast protein liquid chromatography system, and eluted by a 0.5 M imidazole step.

At this stage, wild-type and mutant proteins were pure as checked by electrophoresis on 15% SDS-polyacrylamide gel followed by Coomassie Brilliant Blue R-250 staining and by electrospray mass spectrometry analyses. Purified Srx and Prx were stored at −20 °C in the presence of 20 mM DTT, and 70% $(NH_4)_2SO_4$ and 15% glycerol, respectively, and were stable for several weeks under these conditions. Immediately before use, both proteins were incubated with 50 mM DTT at 4 °C, followed by desalting or oxidation reaction. Protein molar concentrations were determined spectrophotometrically, using extinction coefficients at 280 nm determined experimentally, of 7280 M^{-1} cm^{-1} for wild-type and mutant Srxs, and of 29500 M^{-1} cm^{-1} for wild-type and mutant Prxs. Prx enzymatic activity was measured by a coupled assay using the Trx recycling system (0.5 μM NTR, 200 μM NADPH, 50 μM Trx), with 100 μM H_2O_2 as substrate. Initial rate measurements were carried out at 30 °C in buffer TK (50 mM Tris-HCl, 100 mM KCl, pH 7.0) on a UV mc2 spectrophotometer (Safas, Monaco) by following the decrease of the absorbance at 340 nm due to the oxidation of NADPH. A steady-state rate constant of 2 s^{-1} was measured in these conditions.

Preparation of Overoxidized Prx—Oxidation of Cys C_P of both wild-type and C171A Prxs was achieved in TK buffer at 30 °C, by incubation of 500 μM Prx with 5 mM H_2O_2 in the presence of 100 mM DTT, followed by two additions of 5 mM H_2O_2 at 10-min intervals. The oxidized protein ($PrxSO_2$) was then desalted through an Econo-Pac 10 DG column (Bio-Rad) equilibrated with buffer TK. The sulfinic oxidation state of Cys C_P was checked by titration of the protein with 5,5′-dithiobis(2-nitro)benzoate under denaturing conditions (1% SDS), by following the loss of Prx enzymatic activity and by electrospray mass spectrometry analysis. $PrxSO_2$ molar concentration was determined spectrophotometrically, using extinction coefficients at 280 nm determined experimentally of 27500 M^{-1} cm^{-1} for the wild-type and mutant proteins.

Kinetics of Srx Reaction under Steady-state Conditions—The reaction was followed in the steady state using Trx as reducer and the Trx recycling system as a coupled assay (50 μM Trx, 0.5 μM NTR, and 200 μM NADPH), in the presence of 1 mM ATP, 1 mM $MgCl_2$, 100 μM $PrxSO_2$, and variable concentrations of Srx. Initial rate measurements were carried out at 30 °C in buffer TK on a Safas UV mc2 spectrophotometer by following the decrease of the absorbance at 340 nm due to the oxidation of NADPH. A blank measurement recorded in the absence of Srx was systematically deduced from the assay to account for the nonspecific oxidation of NTR. When wild-type $PrxSO_2$ was used as substrate, a stoichiometry of 2 mol of NADPH per mol of $PrxSO_2$ was used in rate calculations to account for the oxidation of 1 mol of Trx per mol $PrxSO_2$ in Prx own catalytic cycle, following the reduction of Cys C_P to the sulfenic acid state.

SDS-PAGE and Immunoblot Analysis—Reaction mixtures containing 30 μM Srx and 30 μM $PrxSO_2$, 1 mM ATP, 1 mM $MgCl_2$, were incubated in buffer TK for 30 s, 1 min, and 2 min at

30 °C. DTT was added to 50 mM in an additional sample incubated for 2 min. All reactions were then treated by 250 mM IAM, and the proteins were immediately loaded onto 15% SDS-PAGE gel in non-reducing conditions, followed by Coomassie Blue staining. The proteins separated on two additional identical gels run in parallel were transferred on nitrocellulose membranes for revelation with antibodies against Srx or His tag. Immune complexes were detected with horseradish peroxidase-conjugated secondary antibodies and enhanced chemiluminescence reagents (Pierce).

PNP-coupled Assay—The kinetics of P_i release were followed by the decrease of the emission fluorescence intensity associated with the phosphorolysis of ^{m7}Guo catalyzed by PNP as a coupled assay (22). Time courses were recorded at 30 °C on an SX18MV-R stopped-flow apparatus (Applied PhotoPhysics, Leatherhead, UK) fitted for fluorescence measurements, with the excitation wavelength set at 305 nm, and the emitted light was collected above 455 nm using a cutoff filter. One syringe contained 1 mM ATP, 1 mM $MgCl_2$, 300 μM ^{m7}Guo, 5 μM PNP in buffer TK, and the other contained 100 μM $PrxSO_2$, 20 μM PNP, variable concentration of Srx in the presence or absence of 300 μM Trx (final concentrations after mixing). For each condition, a blank time course was recorded in the absence of Srx and deduced from the corresponding experience in the presence of Srx. An average of three runs was recorded for each set of conditions. Under single turnover conditions (in the absence of Trx), the rate constant k_{obs} was obtained by fitting fluorescence traces after blank deduction against Equation 1, in which c represents the end point and a is the amplitude of the fluorescence decrease.

$$y = ae^{-k_{obs}t} + c \qquad \text{(Eq. 1)}$$

The steady-state rate constant was obtained by measurement of initial rate in the presence of Trx. The fluorescence signal was calibrated against P_i concentration to allow determination of the stoichiometry of P_i released during Srx reaction.

Kinetics of Formation of the Prx-Srx Complexes followed by Reverse Phase Chromatography—Reaction mixtures containing 20 μM C48A-C106A Srx and 100 μM C171A $PrxSO_2$, 1 mM ATP, 1 mM $MgCl_2$ were incubated in the TK buffer at 30 °C. Aliquots were quenched by using trifluoroacetic acid, 0.1%, and analyzed by reversed-phase liquid chromatography on an Aquapore RP-300 (C8) column, 4.6 × 100 mm, 7 μm (PerkinElmer Life Sciences), coupled to the ÄKTAexplorer system (Amersham Biosciences), using the same gradient as described below for LC-MS.

Liquid Chromatography Coupled to Mass Spectrometry: Sample Preparation—Reaction mixtures containing 30 μM Srx (C48A-C106A double mutant/wild-type Srx) and 30 μM $PrxSO_2$ (C171A/wild-type $PrxSO_2$), 1 mM ATP, 1 mM $MgCl_2$ were incubated in buffer TK for 30 s, 2 min, and 10 min at 30 °C. Reactions were then treated by 25 mM IAM. Finally, samples were diluted 2.5 times and were analyzed by reversed-phase LC-MS immediately to cope with thiosulfinate instability and to prevent secondary reactions.

LC-MS Analyses—MicroLC-MS analyses were performed on a Hewlett Packard 1100 Series Analytic LC system coupled with a MicrOTOF-Q Mass spectrometer (Bruker Daltonics, Bremen, Germany). An aliquot of 50 μl of each sample was loaded immediately after preparation onto a Vydac 208TP52 (C8) column, 2.1 × 250 mm, 5 μm. Proteins were eluted from the column using a linear gradient from 30 to 60% of B in 30 min and from 60 to 80% of solvent B in 1 min with A:H_2O plus 0.1% trifluoroacetic acid (v/v) and B:acetonitrile plus 0.08% trifluoroacetic acid (v/v) at a flow rate of 250 μl min^{-1}. The column was then flushed with 80% of solvent B during 5 min.

The capillary and end plate voltage of the mass spectrometer were set to −4500 V and −500 V, respectively. The complete system was fully controlled by HyStar and micrOTOFControl software (Bruker Daltonics). For the measurements, external calibration was performed with a horse heart myoglobin solution at 0.2 pmol μl^{-1} in a water/acetonitrile mixture (1:1, v/v) acidified with 1% (v/v) formic acid. The MS acquisition range was set between m/z 500 and 3000, and three scans were averaged to obtain MS spectra. Collected data were treated using DataAnalysis software (Bruker Daltonics). For all spectra, the baseline was subtracted before they were smoothed once using the Savitsky-Golay algorithm with a smoothing width of 0.2 m/z. Deconvoluted mass spectra were performed using the Maximum Entropy Charge Deconvolution module (Bruker Daltonics). Ratios of thiosulfinate and disulfide intermediates were estimated from peak heights of the deconvoluted mass spectra.

High Resolution MS Analysis—To achieve the required resolution to discriminate co-eluting Prx-Srx thiosulfinate and disulfide complexes (mass difference of 16 Da), a fine tuning of the mass spectrometer was performed to get a minimal theoretical mean mass resolution (full width at half-maximum (FWHM)) of 2,350 at 37 kDa. Preliminary experiments performed in the "focus mode" with tuning mix solution (Agilent Technologies, Santa Clara, CA), aiming at maximizing resolution around m/z 1000, allowed to reach a mean resolution (FWHM) of 18,000 for a 15-kDa protein. This optimization subsequently led to a resolution (FWHM) of 2,800 for a 37-kDa protein complex.

Control Experiments—Prior to each reaction monitoring, a control experiment, in the same conditions as those described above but without ATP addition, was performed (see Fig. 3). Mass assignments were performed after LC-MS analysis. The following molecular masses were measured: (i) peak 1′: wild-type Srx plus 2 IAM (13,836.9 ± 0.1 Da); (ii) peak 2′: wild-type $PrxSO_2$ plus IAM (23,711.4 ± 0.1 Da), wild-type PrxSOH plus IAM (23,694.6 ± 0.6 Da), wild-type $PrxSO_2$ (23,654.3 ± 0.3 Da) and wild-type $PrxSO_3$ (23,726.4 ± Da); (iii) peak 3′: wild-type Srx plus 2 IAM (13,835.8 ± 0.1 Da) and wild-type Srx plus IAM (13,778.8 ± 0.2 Da); (iv) peak 5′: C171A $PrxSO_2$ (23,620.1 ± 0.3), C171A PrxSOH (23,603.1 ± 0.5 Da) and C171A $PrxSO_3$ (23,635.5 ± 0.5 Da); (v) peak 7′: C48A/C106A Srx plus IAM (13,715.17 ± 0.4 Da); and (vi) peak 9′: C171A $PrxSO_2$ (23,621.0 ± 0.6 Da), C171A PrxSOH (23,604.1 ± 0.5 Da), and C171A $PrxSO_3$ (23,636.6 ± 0.6 Da).

RESULTS AND DISCUSSION

Identification of Prx-Srx Species Formed in the Absence of Added Reducer—Mechanistic studies on Srxs have been reported for *S. cerevisiae* and mammalian enzymes, including searching for covalent intermediates between overoxidized Prx

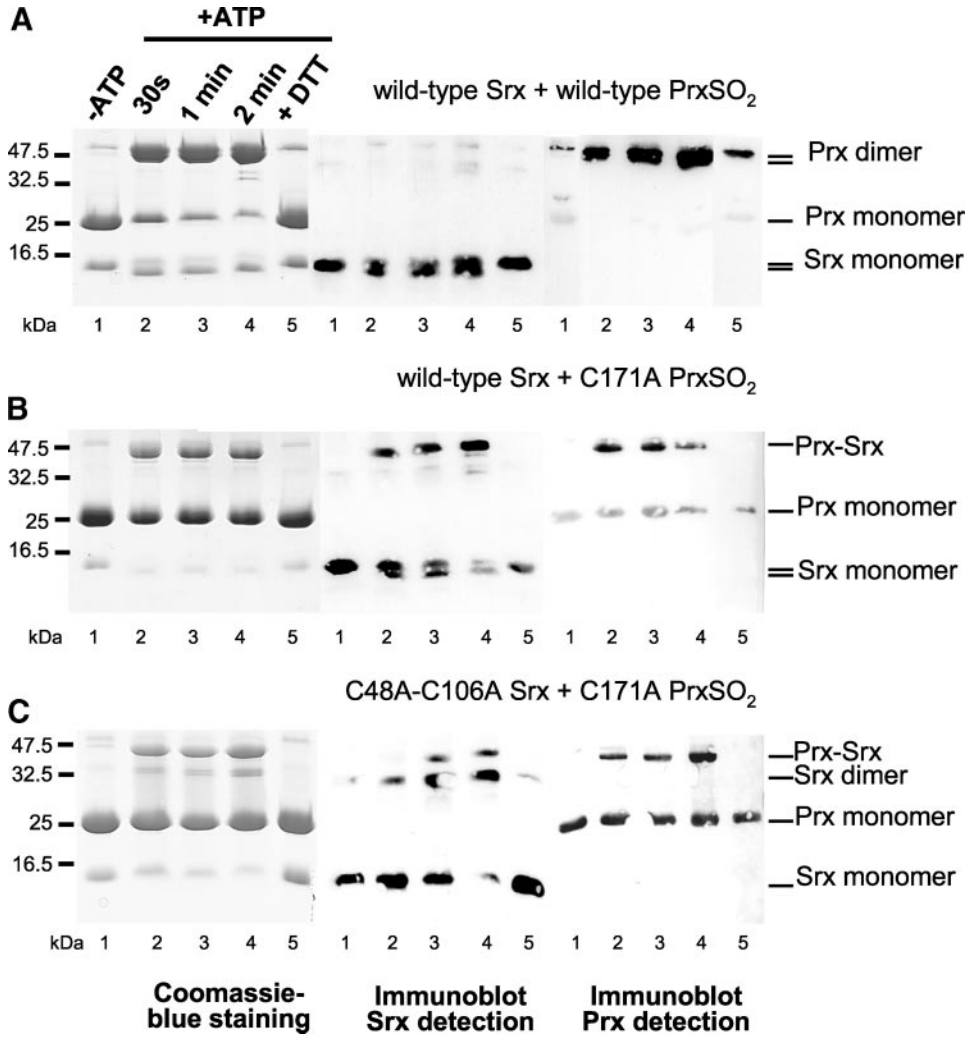

FIGURE 2. **Non-reducing SDS-PAGE and immunoblot analysis of the species formed for the reaction catalyzed by Srx in the absence of added reducer.** Equimolar concentrations (30 μM) of Srx and $PrxSO_2$ were mixed in the absence (*lane 1*) or presence of 1 mM ATP-$MgCl_2$ for the indicated times (*lanes 2–4*), and for 2 min followed by the addition of 50 mM DTT (*lane 5*), immediately followed by addition of 25 mM IAM and non-reducing SDS-PAGE fractionation. Reactions were carried out in TK buffer at 30 °C. Three identical SDS-PAGE gels were run in parallel for Coomassie Blue staining (*left panel*) or immunoblot revelation against Srx (*middle panel*) and His tag (*right panel*) specific antisera. *A*, wild-type $PrxSO_2$ and wild-type Srx; bands corresponding to monomeric Prx in the immunoblot are very faint due to the relative amounts and sensitivity to His tag antisera of both species; *B*, C171A $PrxSO_2$ and wild-type Srx; *C*, C171A $PrxSO_2$ and C48A-C106A Srx.

substrate and Srx enzyme. Studies on *S. cerevisiae* cells subjected to H_2O_2 stress identified a Cys-84-dependent $(Prx)_2$-Srx species with DTT-sensitive linkage in cellular extracts which, although not fully chemically characterized, led to the suggestion that Srx catalytic Cys could be involved in the formation of a Prx-Srx thiosulfinate intermediate species (1). On the contrary, no thiosulfinate species could be detected after *in vitro* reaction of human overoxidized Prx1 and human Srx in the presence of ATP, followed by Western blot and mass spectrometry analyses (17). We therefore tackled the *in vitro* study of the reaction products of *S. cerevisiae* Srx with the His-tagged overoxidized peroxiredoxin Tsa1 (referred to as $PrxSO_2$), shown to interact with Srx *in vivo* (1), in non-reducing conditions to allow the accumulation of intermediate species.

The potential reactivity and instability of the thiosulfinate bond have already been studied on model compounds. In particular, it is known that thiosulfinates react readily with thiols, which are described to attack preferentially on the sulfenic sulfur (-S-) rather than on the sulfinic sulfur (-SO-) of the thiosulfinate bond, giving off a disulfide product and a sulfenic acid product (23, 24). Therefore, we set up experimental conditions aiming at reducing secondary reactions on this putative intermediate. First, the potential secondary reactions of free thiol groups of Srx and Prx with intermediate species in the absence of reducer were avoided during the subsequent analysis steps by carbamidomethylation with IAM, which alkylates the remaining free thiol groups, immediately followed by non-reducing SDS-PAGE or LC-MS. Second, because free thiols of Srx and $PrxSO_2$ could lead to secondary reactions also during the time course of experiments, assays were carried out both on wild-type and C48A-C106A double mutant Srx and both on wild-type and C171A $PrxSO_2$. Indeed, *S. cerevisiae* Srx contains two non-conserved Cys in positions 48 and 106 in addition to the catalytic Cys-84, for which substitutions were described to have minor effects on the reaction *in vivo* (1). Using the C171A mutant $PrxSO_2$, which lacks the regeneration Cys C_R, as a substrate for Srx, gave a similar steady-state rate constant as wild-type $PrxSO_2$ (1.7 ± 0.4 min^{-1} *versus* 1.9 ± 0.4 min^{-1}) in the presence of Trx as reducer by the Trx/NTR assay. This suggests that this residue was not involved in Srx catalytic mechanism, as observed for the human enzyme (17).

The products of the reaction between wild-type Srx and wild-type or C171A $PrxSO_2$ and between C48A-C106A Srx and C171A $PrxSO_2$ in non-reducing conditions were analyzed by SDS-PAGE and Western blots against Srx and His tag antisera, after 30-s, 1-min, and 2-min incubations (Fig. 2). For the wild-type proteins, in the presence of ATP/$MgCl_2$, two major species migrating at ~47 kDa were formed at the expense of the one corresponding to monomeric Prx (23.6 kDa) and were sensitive to DTT (Fig. 2*A*). Immunoblots revealed that these species comprised only the Prx protein, suggesting that dimeric, DTT-reducible Prx species were formed. Srx was found almost exclusively as a monomeric species (13.7 kDa), although it migrated slightly higher than expected with regard to its molecular weight, probably due to its basic character (theoretical pI of 9.2). In addition, two bands with migration similar to mono-

meric Srx were observed in the presence of ATP, suggesting that a significant fraction of the Srx population migrated slightly faster, resulting in the apparent doubling of this band into two bands. Addition of DTT after 2-min incubation restored the population of Srx migrating as observed before ATP addition, suggesting that the band migrating slightly faster corresponded to an oxidized Srx monomer with an intramolecular disulfide bond. When C171A $PrxSO_2$ was used as the substrate with wild-type Srx (Fig. 2*B*), a major DTT-sensitive species migrating at ~45 kDa appeared in the presence of ATP, corresponding to a Prx-Srx species, as revealed by immunoblotting. Again, likely due to Srx basic character, this species migrated significantly higher than expected for a molecular mass of 37.6 kDa. Division of the Srx band into two was also suggested by Coomassie staining and confirmed by immunoblotting against Srx antisera. Similar to the experiment with wild-type $PrxSO_2$, this phenomenon was reversed by DTT treatment. However, no apparent doubling of the monomeric Srx band occurred for the C48A-C106A mutant of Srx incubated with the C171A substrate (Fig. 2*C*), thus supporting the formation of an oxidized Srx monomer with an intramolecular disulfide bond in the case of wild-type Srx. Instead, a new species migrating at ~32 kDa appeared that comprised only Srx, thus indicating the formation of dimeric Srx, whereas in the same conditions, a Prx-Srx species was produced. As observed in previous conditions, both species dissociated in the presence of DTT, indicating covalent linkages involving oxidized Cys residues.

Given that they were produced specifically in the presence of ATP, several hypotheses on the origins of these species can be raised based on the catalytic mechanisms proposed for Srx. First, the formation of oxidized forms of Srx implies chemical activation of Cys-84. This residue could be activated either as a phosphorylated intermediate according to Jeong *et al.* (17), or as a thiosulfinate intermediate (Fig. 1). In the case of wild-type Srx, intramolecular attack of either Cys-48 or Cys-106 would prevail, resulting in a monomeric oxidized species, whereas in the case of C48A-C106A mutant Srx, intermolecular attack of Cys-84 from native Srx would occur concurrently to the catalytic reactions, leading to a dimeric species. In the hypothesis of formation of a PrxSO-SSrx thiosulfinate intermediate, an important point to note is that this reaction would result in release of the reactive sulfenate form of the peroxidatic Cys C_P of Prx. Second, formation of the dimeric Prx species is associated with the presence of Cys-171 (C_R), suggesting the reaction of Cys C_R on the activated Cys C_P of Prx, likewise the regeneration step in the catalytic cycle of any typical 2-Cys-Prx. Species that could play the role of activated Prx are either the phosphorylated, the thiosulfinate intermediates or the oxidized form of Prx with a sulfenate Cys C_P. Two forms, including one or two symmetrical bonds, would be expected, as observed in Fig. 2*A* (*lanes 2–4*) and in a previous study (25). Finally, the Prx-Srx species observed with the C171A mutant of $PrxSO_2$ (Fig. 2, *B* and *C*) can only be explained by the hypothesis involving a PrxSO-SSrx thiosulfinate intermediate: either it corresponds to the intermediate itself, or to a disulfide issued from the reaction of a free thiol of Srx with the sulfenic Prx-C_PSOH released from the thiosulfinate intermediate, as suggested above.

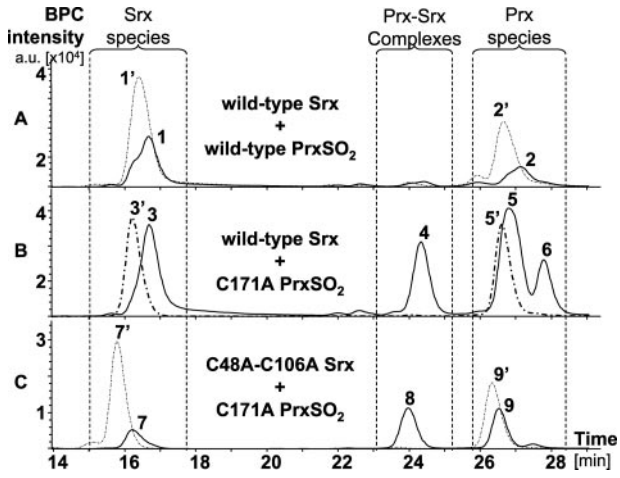

FIGURE 3. **LC-MS analysis of the reaction catalyzed by Srx in the absence of added reducer.** Reactions were carried out for 2 min in the same conditions as in Fig. 2, in the absence (*dashed lines*) and in the presence of ATP (*solid lines*), immediately followed by addition of 25 mM IAM and by LC-MS analysis. Base peak chromatograms of wild-type $PrxSO_2$ and wild-type Srx (*A*), C171A $PrxSO_2$ and wild-type Srx (*B*), and C171A $PrxSO_2$ and C48A-C106A Srx (*C*) are presented. Protein species are eluted in three clusters of peaks corresponding to Srx species, covalent Prx·Srx complexes and Prx species. Peaks are numbered for reference in the text and in Table 1.

Identification of a Thiosulfinate Intermediate by LC-MS and NanoLC-MS/MS Analyses—To test the hypothesis of the formation of a thiosulfinate complex, we focused on the structural characterization of the various products of the reactions between Prx (wild type/C171A mutant) and Srx (wild type/C48A-C106A double mutant) species by LC-MS. To distinguish between possible disulfide and thiosulfinate complexes between Srx and Prx, which are differentiated by a mass increase of 16 Da, a minimal theoretical mean mass resolution (FWHM) of 2,350 at 37 kDa is needed, which implies the use of a mass spectrometer finely tuned for high resolution (see "Experimental Procedures" for details).

Fig. 3 presents base peak chromatograms obtained for control experiments performed in the absence of ATP and for enzymatic reactions run for 2 min in the presence of ATP, in conditions similar as for Western blot analyses. For control experiments (*dashed lines*), two main peaks were detected. MS analysis showed that species eluting at retention times between 15 and 18 min and between 26 and 28 min corresponded to monomeric Srx and to monomeric $PrxSO_2$, respectively, labeled with carbamidomethyl groups inherent to IAM treatment. Molecular masses measured for control experiments (peak numbers 1′, 2′, 3′, 5′, 7′, and 9′) are given under "Experimental Procedures."

In the presence of ATP, one additional peak eluting between 23 and 25 min was observed for reactions involving the C171A $PrxSO_2$ mutant (Fig. 3, *B* and *C*, *solid lines*), which corresponds to Prx-Srx complexes (*peaks 4* and *8*). Mass assignments after LC-MS analyses in the presence of ATP are reported in Table 1. By contrast, for the reaction of wild-type Srx with wild-type $PrxSO_2$, no additional Prx-Srx complex peak was observed on the chromatogram (Fig. 3*A*), which is in agreement with the results of Western blots. *Peak 2* (at retention time ~27 min) revealed two major species, with masses that may be attributed to dimeric Prx linked with one (PrxS-S$PrxSO_2$) or two (PrxS-S/

TABLE 1

Mass assignments obtained after LC-MS analysis for the reaction catalyzed by Srx in the absence of added reducer

Reactions were carried out for 2 min in the same conditions as in Fig. 2, immediately followed by addition of 25 mM IAM and by LC-MS analysis. Minor species (<10%) are not reported, and major ones are in bold. Peak numbers refer to Fig. 3. Data are expressed in daltons.

RT	Species		Wild-type Srx and Prx		Wild-type Srx and C171A Prx		C48A-C106A Srx and C171A Prx	
			Observed molecular mass	Expected molecular mass	Observed molecular mass	Expected molecular mass	Observed molecular mass	Expected molecular mass
min					*Da*			
15–18	**Srx**		**Peak 1**		**Peak 3**		**Peak 7**	
				13,722.7		13,722.7	**13,658.6 ± 0.1**	13,658.6
		+IAM	13,779.6 ± 0.3	13,779.8	13,779.9 ± 0.3	13,779.8	**13,715.5 ± 0.1**	13,715.6
		+2 IAM	13,836.8 ± 0.4	13,836.8	13,836.4 ± 0.7	13,836.8		13,772.6
		SS Bridge	**13,721.0 ± 0.2**	13,720.7	**13,721.1 ± 0.1**	13,720.7		
	Dimer of Srx	SrxS·SSrx		27,443.4		27,443.4	27,316.6 ± 0.7	27,315.2
		+2 IAM		27,557.5		27,525.5	**27,430.6 ± 0.5**	27,429.3
		+4 IAM		27,671.6		27,639.6	27,543.6 ± 0.7	27,543.4
23–25	**Disulfide complex**				**Peak 4**		**Peak 8**	
		PrxS·SSrx		37,342.3		37,310.3	**37,247.3 ± 0.4**	37,246.1
		+IAM		37,399.4	**37,368.7 ± 0.2**	37,367.3		
	Thiosulfinate complex	PrxSO·SSrx		37,358.3		37,326.3	**37,262.6 ± 0.4**	37,262.1
26–29	**Oxidized Prx**		**Peak 2**		**Peak 5**		**Peak 9**	
		$PrxSO_2$	23,654.6 ± 0.5	23,653.6	**23,622.2 ± 0.4**	23,621.5	**23,621.9 ± 0.4**	23,621.5
		$PrxSO_3$		23,669.6	23,638.3 ± 0.1	23,637.5	23,637.6 ± 0.3	23,637.5
	Reduced Prx				**Peak 6**		**Peak 10**	
				23,621.6	**23,590.2 ± 0.2**	23,589.5	23,589.9 ± 0.4	23,589.5
	Dimer of Prx	PrxS·S/S·SPrx	**47,241.5 ± 0.3**	47,239.2		47,177.1		47,177.1
		$PrxS·SPrxSO_2$	**47,277.8 ± 0.7**	47,273.2				
		+IAM	47,338.2 ± 0.6	47,330.2				

S-SPrx) disulfide bonds (Table 1), likely between the Cys C_P and C_R from symmetrical subunits. However, the resolution of the MS instrument at 47 kDa did not allow us to discriminate between these two species. Such a result provides the first evidence in favor of the formation of a thiosulfinate intermediate between Srx and Prx, because it implies the reaction of the Cys C_R on a released sulfenic Prx-C_PSOH species. Therefore, reduction of the sulfinic $PrxSO_2$ is possible by a Srx thiol group in the absence of added reducer. For the reaction of wild-type Srx and C171A $PrxSO_2$, *peak 4* (Fig. 3*B*) corresponds to one single ion series with a measured molecular mass of 37,368.7 ± 0.2 Da (Table 1), which could be attributed to a disulfide PrxS-SSrx complex with one IAM adduct (expected molecular mass of 37,367.3 Da), which is in agreement with Western blot analyses.

Finally, direct evidence in favor of the formation of a thiosulfinate-type PrxSO-SSrx species was obtained by LC-MS analysis of the reaction of the C48A-C106A double mutant Srx and C171A $PrxSO_2$. Indeed, MS analysis of peak 8 complexes showed a mixture of two species (Fig. 3*C*, Table 1): i) a compound with a mass of 37262.6 ± 0.4 Da which could correspond to the expected PrxSO-SSrx thiosulfinate complex (expected MW: 37262.1 Da, see Table 1) and ii) a species with a mass of 37247.3 ± 0.4 Da which could be attributed to the PrxS-SSrx disulfide complex (expected MW: 37246.1 Da, see Table 1). Since Srx Cys-84 and Prx C_P are the only Cys residues available for the reaction, this result strongly argues in favor of the accumulation of a PrxSO-SSrx thiosulfinate species involving Srx Cys-84 and Prx C_P in these conditions.

Even if the most probable explanation for the 37,262-Da species detected by LC-MS is the formation of the thiosulfinate intermediate, another hypothesis cannot be ruled out at this stage. Indeed, the 37,262-Da species could also correspond to a PrxS-SSrx disulfide compound with an additional oxidation of a non-Cys residue. However, LC-MS-monitored kinetic evolution of the ratio of putative thiosulfinate *versus* disulfide species contained in *peak 8* invalidates this hypothesis. Indeed, the fraction of the 37,262-Da complex, which constitutes the major Prx-Srx species after 30-s reaction, decreased with time while the fraction of disulfide PrxS-SSrx species increased (Fig. 4). If the 37,262-Da species was a disulfide, the additional oxidation located for example on a Met residue, could not be reduced in these *in vitro* conditions to produce the PrxS-SSrx species. On the contrary, the evolution observed in Fig. 4 could be explained by the release of PrxSOH from a thiosulfinate species, followed by the attack of a reduced Cys thiol from Srx, which would lead to the increase of the disulfide species. In addition, these reactions would produce a disulfide SrxS-SSrx species. Indeed, such a complex was observed by immunoblotting (Fig. 2*C*) and by LC-MS (*peak 7*, Fig. 3*C*, Table 1). Although no free Cys is available on the SrxS-SSrx dimer, it was observed with two and four carbamidomethyl adducts, which can probably be attributed to increased His and Met reactivity toward IAM for this mutant Srx (26, 27).

To further establish the chemical nature of the bridging bond, *peak 8* was collected after LC-MS analysis and submitted to enzymatic digestions, followed by subsequent tandem mass spectrometry (MS/MS) analysis (see supplemental materials). First, these conditions allowed us to unambiguously confirm the existence of the peptide corresponding to the 74–86 $(GQTLYYAFGGCHR)_2$ disulfide dipeptide of the SrxS-SSrx dimer (see supplemental Fig. S1). Because the digestions were performed on the isolated complexes from *peak 8*, this species can only be explained by the release of free reduced Srx, and it thus implies the hydrolysis of a thiosulfinate species. Indeed, model thiosulfinate compounds have been shown to be sensitive to hydrolysis at neutral or basic pH. Although the mechanism of thiosulfinate hydrolysis appears more complex than nucleophilic attack by thiols, it would significantly involve release of reduced Srx and $PrxSO_2$ as an initial step (28, 29). This result again supports the thiosulfinate nature of the 37,262-Da species. In addition, the dipeptide resulting from the PrxS-SSrx

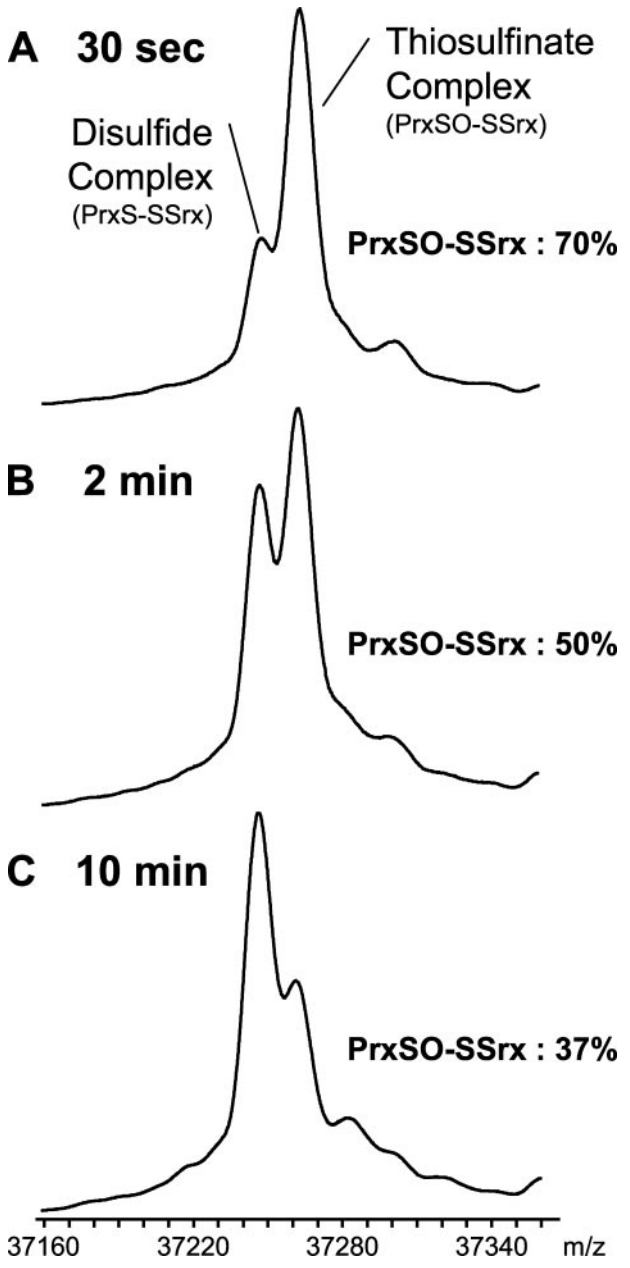

FIGURE 4. **Kinetic evolution of the ratio of thiosulfinate *versus* disulfide complexes monitored by MS.** Deconvoluted mass spectra of the covalent species formed between C171A $PrxSO_2$ and C48A-C106A Srx in the presence of ATP (*peak 8*, Fig. 3) obtained after 30 s (*A*), 2 min (*B*), and 10 min (*C*) reaction in identical conditions as in Fig. 2*C*.

species was also detected, showing the cross-linking of Prx Cys C_P and Srx Cys-84. Indeed, the ion at *m*/*z* 887.65 corresponds to the 5+ charge state of the 54–80 YVVLAFIPLAFTFVCPTEIIAFSEAAK Prx peptide cross-linked by a disulfide bond to the 74–86 GQTLYYAFGGCHR Srx peptide (see supplemental Fig. S2). Due to the instability of thiosulfinate bonds at near neutral pH, no tryptic peptide containing a thiosulfinate cross-link was detected by nanoLC-MS/MS.

To attempt to directly characterize the putative thiosulfinate intermediate, pepsin digestions were performed at acidic pH, which is expected to stabilize the thiosulfinate bond (28). Despite accurate mass measurement of pepsic peptides, no peptide containing either the disulfide or the thiosulfinate bond could be unambiguously sequenced even if molecular masses that could correspond to such peptides were measured with a high accuracy. Two reasons can account for this failure: (i) pepsin is a highly aspecific enzyme, and thus numerous missed cleavages can be considered resulting in a high number of potential theoretical proteolytic peptides, and (ii) MS/MS data for pepsic peptides were of low quality, which made precise sequence determination impossible.

However, analysis of the enzymatic digestions of the complexes by nanoLC-MS/MS allowed us to unambiguously localize the putative thiosulfinate bond on the amino acid scaffold. Indeed, the only peptides that could not be detected after enzymatic digestion (trypsin or pepsin) correspond to peptides containing either Prx Cys C_P or Srx Cys-84 (see supplemental Fig. S3). When reduction (DTT) and alkylation (IAM) treatment was performed before tryptic digestion, the 74–86 GQTLYYAFGGC_{Cam}HR peptide corresponding to the Srx Cys-84-containing peptide was clearly detected and sequenced by nanoLC-MS/MS analysis (supplemental Fig. S4). Even if the corresponding Prx Cys C_P-containing peptide could not be observed after trypsin digestion, it could be sequenced in acidic conditions after pepsin digestion (supplemental Fig. S5).

Based on the preceding results, we propose the following scenario to explain the evolution of the reaction products (Fig. 5): formation of a thiosulfinate intermediate between Srx Cys-84 and Prx Cys C_P occurs first after activation of Prx by phosphorylation. All secondary products derive from the high reactivity of this species, in particular toward thiols. For the reaction of C48A-C106A double mutant Srx with C171A $PrxSO_2$ (Fig. 5*B*), reduced Srx, resulting from the hydrolysis of the thiosulfinate intermediate, would attack the sulfenate sulfur of the thiosulfinate intermediate, producing dimeric oxidized Srx (*peak 7*, Figs. 3*C* and 5*B*) and $PrxC_PSOH$. $PrxC_PSOH$ would then react rapidly with reduced Srx, generating the PrxS-SSrx species observed in *peak 8* (Figs. 3*C* and 5*B*). Finally, a second attack of reduced Srx on the PrxS-SSrx disulfide complex would then result in the formation of a small amount of reduced Prx observed (*peak 10*, Fig. 3*C*, Table 1, and Fig. 5*B*). Reduced Prx was no longer observed after 10-min incubation (data not shown), likely due to the formation of a mixed disulfide with reduced Srx.

For wild-type Srx (Fig. 5*A*), the hypothesis of an intramolecular attack of a non-catalytic Cys thiol on Cys-84 sulfur atom is supported both by the electrophoretic shift of the monomeric Srx band (Fig. 2) and by LC-MS analysis. Indeed, a species at 13,721.0 ± 0.2 Da, corresponding to a decrease of 2 Da compared with the expected molecular mass for Srx (13,722.7 Da, see Table 1) was observed in *peaks 1* and *3* when wild-type Srx reacts with wild-type and C171A $PrxSO_2$, respectively (Fig. 3, *A* and *B*). Such an intramolecular disulfide bond was not detected for the reaction of C48A-C106A Srx double mutant with C171A $PrxSO_2$. Alternatively, the hypothesis of an intramolecular attack of a non-catalytic Cys on the putative cysteinyl-phosphate intermediate (Fig. 1*B*) cannot be definitely ruled out. The highly reactive sulfenic species $PrxC_PSOH$ then rapidly evolved (within 30-s incubation, data not shown) into dimeric disulfide Prx species (*peak 2*, Fig. 3*A*) in the presence of the regeneration Cys C_R (Fig. 5*A*). Indeed, this reaction is part of

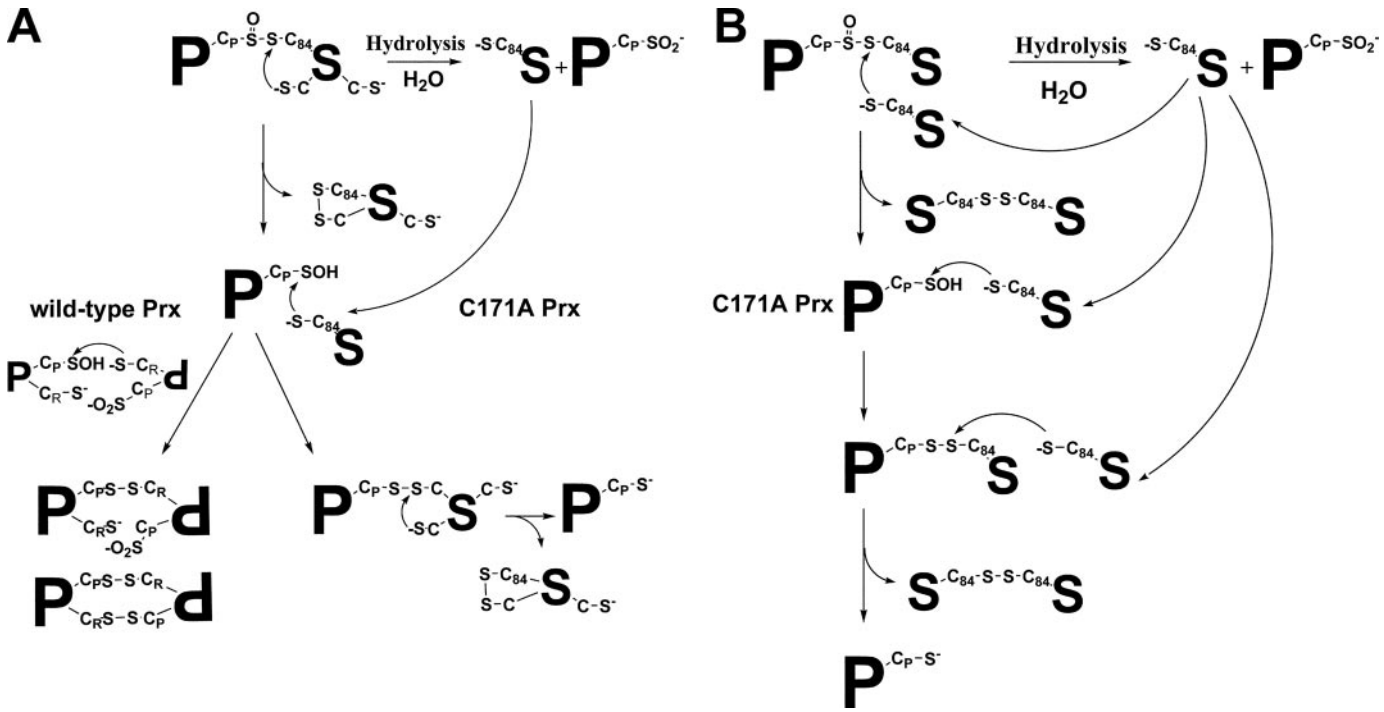

FIGURE 5. **Proposed scenario for the evolution of the thiosulfinate species.** Secondary reactions are deduced from SDS-PAGE, immunoblot, and LC-MS analysis of the reaction of wild-type Srx with wild type and C171A $PrxSO_2$ (*A*) and of C48A-C106A mutant Srx with C171A mutant $PrxSO_2$ (*B*), run in the conditions of Fig. 2.

the catalytic cycle of the peroxidase, at rates at least 50 times higher than Srx (rate constants of 2 s^{-1} *versus* 1.8 min^{-1}). When the regeneration Cys of Prx is mutated, the residual free thiols are carried only by Srx, which explains the formation of intermolecular mixed disulfide PrxS-SSrx as secondary species (*peak 4*, Fig. 3*B*). If hydrolysis of the thiosulfinate is significant during the time scale of the reaction, release of reduced Srx could provide the free thiol groups (Fig. 5*A*). Two arguments support the later proposition: first, the disulfide PrxS-SSrx species is labeled by IAM and thus cannot arise from reaction of the remaining Cys of oxidized Srx released, and second, there is formation of a significant amount of reduced Prx (Fig. 3*B*, *peak 6*, and Table 1) in less than 30 s (data not shown). This probably results from an intramolecular attack of a thiol of Srx on the PrxS-SSrx disulfide linkage, similar to the reaction taking place within the thiosulfinate intermediate (Fig. 5*A*). Therefore, no significant reaction would occur between the released Prx sulfenate and the remaining thiol of oxidized Srx, which suggests that recognition between both partners is needed for efficient attack of Srx catalytic Cys-84 on Prx Cys C_P. In addition, a significant hydrolysis of the thiosulfinate complex would also explain why a substantial fraction of $PrxSO_2$ is left non-reacted, as visible both on SDS-PAGE (Fig. 2, *B* and *C*) and by LC-MS (Fig. 3, *peaks 2*, *5*, and *9*, and Table 1).

Kinetic Analysis of the Formation of the Prx-Srx Species—Because all products of the reactions between the wild-type and mutant forms of both Srx and $PrxSO_2$ can be explained by the formation of a thiosulfinate PrxSO-SSrx complex, the question arises of the relevance of this species as an intermediate in the catalytic pathway. We addressed this question by a kinetic approach for real-time monitoring of the formation of this species by the production of P_i. For this purpose, we used the PNP coupled assay, which monitors the decrease of fluorescence upon phosphorolysis of ^{m7}Guo. The assay was validated in the steady-state conditions by comparison with the Trx/NTR coupled assay in the presence of Trx as the reducing agent, which gave a rate constant of 1.7 ± 0.2 min^{-1} for wild-type $PrxSO_2$, similar to 1.9 min^{-1} for the Trx/NTR assay using saturating/optimal concentrations of $PrxSO_2$, ATP, $MgCl_2$, and Trx. This value was also confirmed by a method based on the titration of the product of the Srx reaction, *i.e.* reduced Prx, by following the regeneration of its peroxidase activity in the presence of 10 mM DTT as electron donor, which gave a slightly slower steady-state rate constant of 1.5 ± 0.1 min^{-1}.

Each of the reactions analyzed previously by Western blot and LC-MS was followed by the PNP assay. Single turnover conditions were used, *i.e.* absence of reducer and excess $PrxSO_2$ relative to Srx, to allow the determination of the rate constant and stoichiometry of formation of the intermediate relative to Srx. If the formation of the intermediate is part of the catalytic pathway, the rate constant of the reaction is expected to be at least equal to the steady-state rate constant, and the amplitude of the reaction should be equal to the limiting concentration, *i.e.* Srx. Indeed, depending on the relative rates of the secondary reactions following the formation of thiosulfinate, the species that accumulates will be either the intermediate itself, or an oxidized form of Srx (Fig. 5). Furthermore, one advantage of this method is to "filter off" secondary reactions such as formation of the disulfide species Prx-Srx, which are not monitored by the PNP assay.

The kinetics recorded for the reaction of wild-type Srx with wild-type and C171A $PrxSO_2$ gave very similar results. In the absence of Srx, a nonspecific linear phosphate release was measured, at a rate constant of ~0.015 min^{-1}. After subtrac-

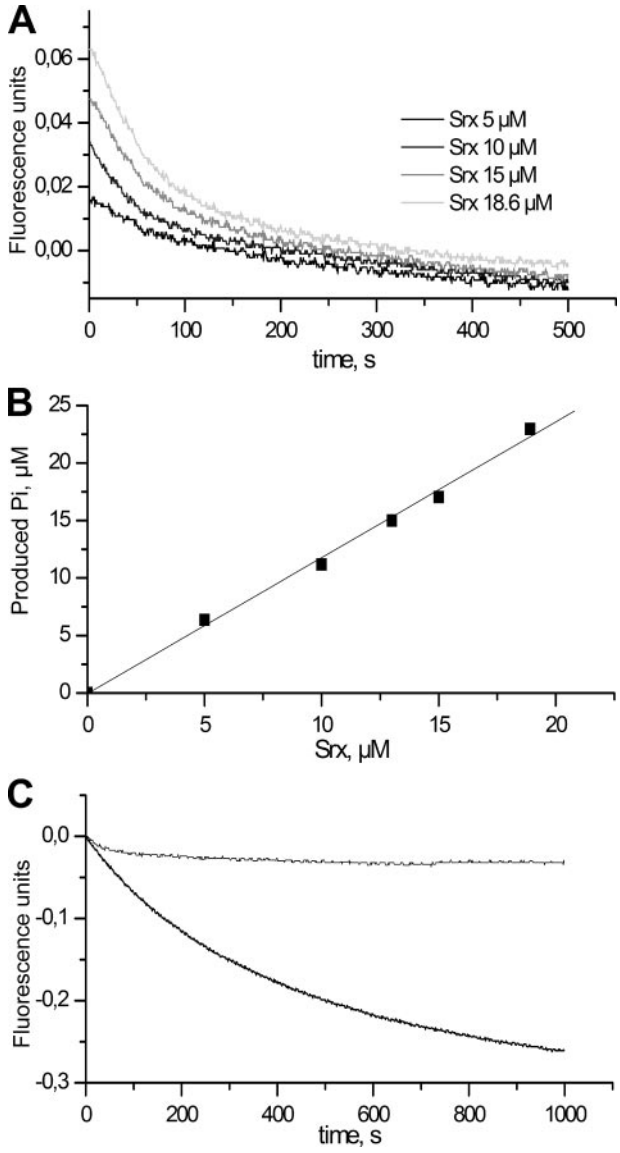

FIGURE 6. **Kinetics of the reaction catalyzed by wild-type Srx with wild-type $PrxSO_2$ monitored by P_i release.** *A*, the reaction of 100 μM wild-type $PrxSO_2$ with variable concentrations of wild-type Srx (5, 10, 15, and 18.6 μM) in the presence of 1 mM ATP/$MgCl_2$ was monitored on a rapid kinetics spectrofluorometer by the PNP coupled assay (see text). Reactions were carried out in TK buffer at 30 °C. The progress curves are corrected from blank traces collected in the absence of Srx. *B*, stoichiometry of P_i produced as a function of Srx concentration deduced from the amplitude of the time courses from *panel A* analyzed as monoexponential processes, and from a calibration curve of the fluorescence signal against P_i established in identical conditions. *C*, comparison of the kinetics of P_i release for the reaction of wild-type Srx (5 μM) with 100 μM wild-type $PrxSO_2$ in the presence of 1 mM ATP/$MgCl_2$, in the presence (*thick line*) or absence (*thin line*) of 300 μM Trx.

tion from the traces collected in the same conditions in the presence of increasing concentrations of Srx, the resulting progress curves were best described by a monoexponential equation, corresponding to a first order process, characterized by a rate constant of 1.8 ± 0.7 min^{-1} independent of Srx concentration (Fig. 6*A*). This rate constant is equal to the steady-state rate constant of the Srx-catalyzed reaction measured in the presence of a thiol reducer (1.7 ± 0.2 min^{-1}). Furthermore, the fluorescence response of ^{m7}Guo phosphorolysis was calibrated against phosphate (see "Experimental Procedures"), which

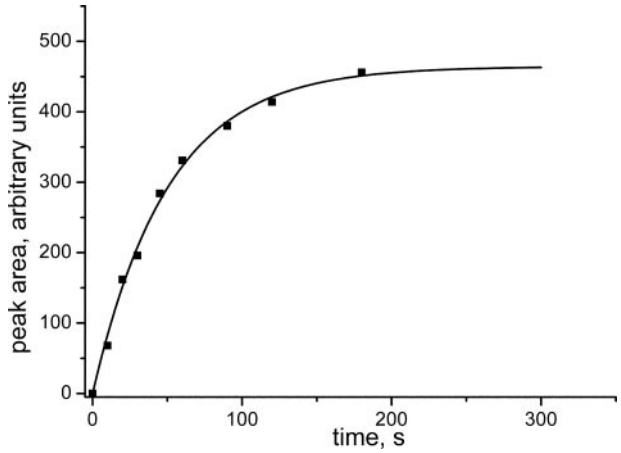

FIGURE 7. **Kinetics of the reaction catalyzed by C48A-C106A Srx with C171A $PrxSO_2$ monitored by reversed-phase chromatography.** The reaction of 100 μM C171A $PrxSO_2$ with 20 μM C48A-C106A Srx in the presence of 1 mM ATP and $MgCl_2$ at 30 °C was followed by analysis of aliquots of the reaction mixture quenched by acidification in trifluoroacetic acid 0.1%, on reversed-phase chromatography with the same gradient as in Fig. 3, monitored by absorption spectrophotometry at 215 nm. The evolution of the area of the peak corresponding to the Prx·Srx complexes (see Fig. 3*B*, *peak 8*) is plotted as a function of time (*dots*) and analyzed by a monoexponential kinetic model (*solid line*) with a rate constant of 1.2 ± 0.1 min^{-1}.

allowed the analysis of the amplitude of the process as a function of Srx concentration. As shown on Fig. 6*B*, the reaction occurs with a stoichiometry of 0.96 ± 0.16 mol of P_i released per mol of Srx. These results support the accumulation of an intermediate species, the stoichiometry of which is limited by Srx concentration, at a rate compatible with catalysis. On the contrary, the amount of P_i released in the presence of an excess of Trx was compatible with the initial concentration of $PrxSO_2$ in the assay (Fig. 6*C*). Therefore, formation of the thiosulfinate species is strongly supported as a specific step on the catalytic pathway. In addition, the similarity between the rate constant measured in single turnover conditions and in steady-state conditions indicates that the rate-limiting step of the overall reaction occurs before or at this step. The kinetics of the reaction of C48A-C106A Srx with C171A $PrxSO_2$ revealed a similar behavior in the absence of reducer, with a rate constant of P_i release of 2.0 ± 0.1 min^{-1} independent of Srx concentration (data not shown). A slightly higher stoichiometry of P_i release of 1.3 mol of P_i released per mol of Srx was observed. This supports hydrolysis of the thiosulfinate intermediate, as hypothesized above, which would result in 30% additional catalytic cycles in addition to the secondary reactions on the thiosulfinate intermediate already described (Fig. 5*B*).

To confirm the catalytic intermediacy of the thiosulfinate species, we followed the kinetics of evolution of the area of the chromatographic peak corresponding to peak 8 (Fig. 3*C*), after reaction of C48A-C106A Srx with C171A $PrxSO_2$ in the presence of ATP, monitored by UV spectrophotometry. Indeed, we showed that this peak contains two species, the putative thiosulfinate PrxSO-SSrx and the disulfide PrxS-SSrx which, assuming the scenario proposed in Fig. 5*B*, should derive from the secondary reactions of the thiosulfinate species. Therefore, the kinetics of evolution of the area of this peak should approximate the kinetics of production of the PrxSO-SSrx species. As shown in Fig. 7, this follows monoexponential kinetics with a

rate constant of 1.2 ± 0.1 min^{-1} close to the rate of P_i release. Such results again support the role of the Prx-Srx species with a mass corresponding to a thiosulfinate as a catalytic intermediate. The slightly lower rate constant measured by chromatography can probably be attributed to the evolution of this reactive species by the side reactions described Fig. 5*B*.

This interpretation raises the problem of the compatibility of the results obtained on *S. cerevisiae* (this study) and mammalian Srx (17). In their study on human Srx, Jeong *et al.* did not detect an Srx-Prx thiosulfinate species, but a disulfide species between the human Srx catalytic Cys and the regeneration Cys C_R of the Prx. The Prx protein exists in solution as an obligate dimer, or decamer. Because experiments were conducted on the wild-type substrate $PrxSO_2$, this species could result from the attack of Cys C_R from the symmetrical Prx monomer on the sulfenyl sulfur of the thiosulfinate bond, a reaction favored by the existence of the complex. After a 10-min reaction, the greater part of the thiosulfinate intermediate would have reacted to give the disulfide species observed. In addition, it would release Prx with a Cys C_P as a sulfenate, which can react with the catalytic Cys-99 of another human Srx molecule to eventually produce the Prx-$(Srx)_2$ species, the second most abundant form in the experiment shown in Jeong *et al.*, study (17). This interpretation was supported by a control experiment performed on the equivalent reaction for the *S. cerevisiae* proteins, using C48A-C106A Srx and wild-type $PrxSO_2$ for 5 min in the presence of ATP/$MgCl_2$. LC-MS analyses revealed a complex mix, including three chromatographic peaks in addition to the peaks of Srx and Prx, corresponding to mixed disulfide species formed between Prx and Srx (1:1 and Srx 1:2 complexes) and $PrxSO_2$ and Srx (1:1 complex) (data not shown). The authors also reported that these species were formed nonspecifically between Srx and reduced Prx, a result that we also observed in the yeast system (data not shown). However, for the reaction between the substrate $PrxSO_2$ and *S. cerevisiae* Srx, no Prx-Srx species was produced in the absence of ATP (Fig. 2), clearly supporting that the thiosulfinate species observed in this study is specifically formed along the catalytic mechanism.

Kinetics of P_i release for the reaction of human Srx and sulfinic Prx in the absence of reducer were characterized by a stoichiometry largely higher than Srx concentration (17). They were described as a linear phase interpreted as a futile cycle of hydrolysis of the phosphorylated substrate, followed by inactivation of Srx from the nonspecific reaction between the catalytic Cys and Cys C_R of the substrate. However, as proposed above, thiosulfinate hydrolysis would also lead to a futile cycle of recycling of the sulfinic acid substrate and Srx. The kinetics of P_i release for human Srx in the absence of reducer could correspond to hydrolysis. As shown for the yeast system, secondary reactions of hydrolysis and reaction with thiols could compete with the slow formation of the thiosulfinate intermediate (the rate constant for the reaction catalyzed by mammalian Srx is reported to be of 0.2–0.5 min^{-1} (16, 17)). Therefore, for human Srx, either the rate of formation of the thiosulfinate intermediate would be too slow to be resolved from the process of thiosulfinate hydrolysis, or the technique of P_i detection on the hour time scale employed by Jeong *et al.* could not resolve the kinetics of formation of the thiosulfinate (on the minute time scale for yeast Srx) and of secondary reactions.

CONCLUSION

In the present study, the role of Srx as a reductase has been proven by three types of arguments from the analysis of the Srx reaction in the absence of added reducers: first, the observation of the transient formation of a DTT-reducible species with a mass compatible with the thiosulfinate intermediate postulated in Fig. 1*A*, second, the analysis of the different species formed in secondary reactions, which implies obligatory transit through such an intermediate, and finally, the kinetics and stoichiometry of the reaction indirectly monitored in real-time by the release of P_i, or directly by the evolution of the Prx-Srx complex chromatographic peak, which authenticated this species as a catalytic intermediate. Such an interpretation can probably be extrapolated to the catalytic mechanism of Srx from mammals for which no such results were obtained in a previous study by Jeong *et al.* (17), likely due to secondary reactions of the regeneration Cys of the Prx substrate on the thiosulfinate intermediate.

This interpretation implies the attack of Srx catalytic Cys on the phosphorylated Prx substrate, which therefore requires precise recognition and positioning of the reacting Cys from both partners at distances compatible with the chemical steps. Observations from this study, and substrate specificity of Srx for the class of the typical 2-Cys-Prx (6), are in agreement with these conclusions. Furthermore, when this report was under submission, the structure of an artificial human PrxS-SSrx disulfide complex was published (30). This structure strongly supports the formation of a covalent Prx-Srx intermediate involving Prx Cys C_P and Srx catalytic Cys, through the local unfolding of Prx active site triggered by Srx binding. The complex is also stabilized by an interaction with the unfolded C-terminal tail of Prx acting as an embrace onto the Srx molecule.

In addition, catalysis of the ATP-dependent activation of $PrxSO_2$ as a phosphorylated intermediate remains to be elucidated for *S. cerevisiae* Srx. In this regard, the hypothesis of the existence of a phosphorylated Srx intermediate (Fig. 1*B*) is not supported by the structural data on the PrxS-SSrx complex (30). The importance of an Asn residue in position 186 from the Prx was suggested for the human enzyme (31). The role of the corresponding Thr residue in Prx will require further investigation at the chemical level. Finally, the results obtained with wild-type Srx from *S. cerevisiae*, showing the release of oxidized Srx with intramolecular disulfide bond, raise the question of the potential role of the non-catalytic Cys residues of Srx Cys-48 and Cys-106, which are not conserved in human Srx.

Acknowledgments—We thank J. Ugolini and S. Alaoui for excellent technical assistance and Prof. S. Boschi-Muller, Dr. A. Gruez, Dr. H. Mazon, and Dr. C. Schaeffer-Reiss for helpful discussions.

REFERENCES

1. Biteau, B., Labarre, J., and Toledano, M. B. (2003) *Nature* **425,** 980–984
2. Budanov, A. V., Sablina, A. A., Feinstein, E., Koonin, E. V., and Chumakov, P. M. (2004) *Science* **304,** 596–600
3. Rhee, S. G., Kang, S. W., Jeong, W., Chang, T. S., Yang, K. S., and Woo,

H. A. (2005) *Curr. Opin. Cell Biol.* **17,** 183–189
4. Sundaresan, M., Yu, Z. X., Ferrans, V. J., Irani, K., and Finkel, T. (1995) *Science* **270,** 296–299
5. Rhee, S. G. (2006) *Science* **312,** 1882–1883
6. Woo, H. A., Jeong, W., Chang, T. S., Park, K. J., Park, S. J., Yang, J. S., and Rhee, S. G. (2005) *J. Biol. Chem.* **280,** 3125–3128
7. Kang, S. W., Rhee, S. G., Chang, T. S., Jeong, W., and Choi, M. H. (2005) *Trends Mol. Med.* **11,** 571–578
8. Chang, T. S., Jeong, W., Choi, S. Y., Yu, S., Kang, S. W., and Rhee, S. G. (2002) *J. Biol. Chem.* **277,** 25370–25376
9. Wood, Z. A., Poole, L. B., and Karplus, P. A. (2003) *Science* **300,** 650–653
10. Vivancos, A. P., Castillo, E. A., Biteau, B., Nicot, C., Ayte, J., Toledano, M. B., and Hidalgo, E. (2005) *Proc. Natl. Acad. Sci. U. S. A.* **102,** 8875–8880
11. Jang, H. H., Lee, K. O., Chi, Y. H., Jung, B. G., Park, S. K., Park, J. H., Lee, J. R., Lee, S. S., Moon, J. C., Yun, J. W., Choi, Y. O., Kim, W. Y., Kang, J. S., Cheong, G. W., Yun, D. J., Rhee, S. G., Cho, M. J., and Lee, S. Y. (2004) *Cell* **117,** 625–635
12. Findlay, V. J., Townsend, D. M., Morris, T. E., Fraser, J. P., He, L., and Tew, K. D. (2006) *Cancer Res.* **66,** 6800–6806
13. Liu, X. P., Liu, X. Y., Zhang, J., Xia, Z. L., Liu, X., Qin, H. J., and Wang, D. W. (2006) *Cell Res.* **16,** 287–296
14. Glauser, D. A., Brun, T., Gauthier, B. R., and Schlegel, W. (2007) *BMC Mol. Biol.* **8,** 54–67
15. Diet, A., Abbas, K., Bouton, C., Guillon, B., Tomasello, F., Fourquet, S., Toledano, M. B., and Drapier, J.-C. (2007) *J. Biol. Chem.* **282,** 36199–36205
16. Chang, T. S., Jeong, W., Woo, H. A., Lee, S. M., Park, S., and Rhee, S. G. (2004) *J. Biol. Chem.* **279,** 50994–51001
17. Jeong, W., Park, S. J., Chang, T. S., Lee, D. Y., and Rhee, S. G. (2006) *J. Biol. Chem.* **281,** 14400–14407
18. Mulrooney, S. B. (1997) *Protein Expr. Purif.* **9,** 372–378
19. Mossner, E., Huber-Wunderlich, M., and Glockshuber, R. (1998) *Protein Sci.* **7,** 1233–1244
20. Miroux, B., and Walker, J. E. (1996) *J. Mol. Biol.* **260,** 289–298
21. Studier, F. W. (2005) *Protein Expr. Purif.* **41,** 207–234
22. Banik, U., and Roy, S. (1990)) *Biochem. J.* **266,** 611–614
23. Kice, J. L., and Liu, C.-C. A. (1979) *J. Org. Chem.* **44,** 1918–1923
24. Kice, J. L., and Rogers, T. E. (1974) *J. Am. Chem. Soc.* **96,** 8015–8019
25. Chae, H., Uhm, T., and Rhee, S. (1994) *Proc. Natl. Acad. Sci. U. S. A.* **91,** 7022–7026
26. Veniamin, N., Lapko, D. L. S., and Smith, J. B. (2000) *J. Mass Spectrom.* **35,** 572–575
27. Lundell, N., and Schreitmuller, T. (1999) *Anal. Biochem.* **266,** 31–47
28. Nagy, P., and Ashby, M. T. (2007) *Chem. Res. Toxicol.* **20,** 1364–1372
29. Kice, J. L., and Rogers, T. E. (1974) *J. Am. Chem. Soc. U. S. A.* **96,** 8009–8015
30. Jonsson, T. J., Johnson, L. C., and Lowther, W. T. (2008) *Nature* **451,** 98–101
31. Lee, D. Y., Park, S. J., Jeong, W., Sung, H. J., Oho, T., Wu, X., Rhee, S. G., and Gruschus, J. M. (2006) *Biochemistry* **45,** 15301–15309